Modal cutoff in microstructured optical fibers

Boris T. Kuhlmey

School of Physics, University of Sydney, Sydney, NSW 2006, Australia, and
Institut Fresnel, Unité Mixte de Recherche du Centre National de la Recherche Scientifique 6133,
Faculté des Sciences et Techniques de Saint Jérôme, 13397 Marseille Cedex 20, France

Ross C. McPhedran and C. Martijn de Sterke

School of Physics, University of Sydney, Sydney, NSW 2006, Australia

We analyze the nature of modal cutoff in microstructured optical fibers of finite cross section. In doing so, we reconcile the striking endlessly single-mode behavior with the fact that in such fibers all propagation constants are complex. We show that the second mode undergoes a strong change of behavior that is reflected in the losses, effective area, and multipolar structure. We establish the parameter subspace in which the fibers are single mode and an accurate value for the limit of the endlessly single-mode regime. © 2002 Optical Society of America

OCIS codes: 060.2270, 060.2280, 060.2400, 060.2430.

One of the earliest known and most exciting properties of microstructured optical fibers (MOFs) is that they can be endlessly single mode.[1] However, this property was discovered in a pioneering study[1] based on a simple model that is incapable of accurately determining the parameter space in which such an endlessly single-mode regime occurs or of proving with absolute certainty that such a regime exists in real fibers. Recently Mortensen[2] suggested a phase diagram of single-mode operation based on the observation of the evolution of the effective area of the second mode, established with a supercell method. Although that research is of great interest, several limitations still have to be overcome: The suggested diagram was established with a restricted number of points in a narrow region of parameter space, and the effects of the finite cross section of the fibers such as geometrical losses and cladding resonances could not be explored.

In conventional fibers the concept of mode number is well defined[3] in that, for a given geometry and wavelength, a finite set of bound modes has a real propagation constant β, with all others having complex β. By contrast, all modes of MOFs with a finite set of confining holes have complex β.[4–6] This is true even if, as here, the MOFs are modeled as air holes in a lossless material, because the complex nature of β is associated with losses that are due to the finite geometry of confining holes. It is thus of great interest to explore whether the properties of MOF modes permit the establishment of a clear criterion for bound modes, replacing the requirement that β be real. The effective area criterion used by Mortensen[2] with periodic boundary conditions is valuable but can address only geometrical mode properties rather than the energy transport characteristics. Furthermore, the use of periodic boundary conditions leads to an artificial constraint (the area of the unit cell) that limits the divergence of the mode area at cutoff.

We investigate here MOFs in silica at a wavelength of $\lambda = 1.55$ μm (refractive index, 1.444024), for mi-crostructures consisting of 4, 6, 8, and 10 rings of hexagonally packed circular holes of diameter d, with pitch Λ. Each MOF has a single central defect, consisting of a missing hole. We use a recently developed multipole method[4,5] that has the unique ability to calculate both the modes and their losses accurately.

In Fig. 1,[7] we show the imaginary part of n_{eff}:

$$\text{Im}(n_{\text{eff}}) = \text{Im}(\beta/k_0), \tag{1}$$

where β is the complex propagation constant and k_0 is the free-space wave number, for the second mode in a MOF with 8 rings (216 holes). Note that the multipole method determines this quantity to five figures or better if $\text{Im}(n_{\text{eff}}) > 10^{-10}$ and to at least two figures for the whole of Fig. 1.[4,5] At a wavelength λ (in micrometers), $\text{Im}(n_{\text{eff}})$ is linked to the geometrical losses $\mathcal{L}$ (in decibels per kilometer) through
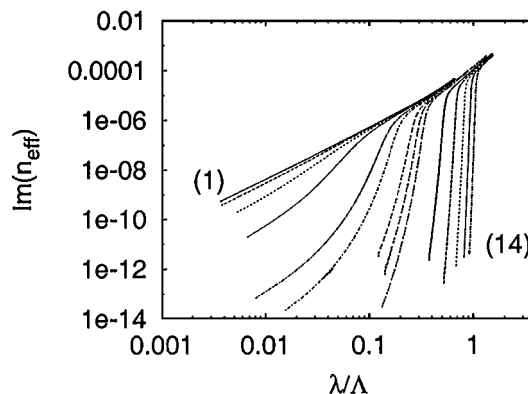

Fig. 1. $\text{Im}(n_{\text{eff}})$ as a function of wavelength/pitch, for a structure of eight rings of holes in silica at a wavelength of $\lambda = 1.55$ μm for several diameter-to-pitch ratios. $I(n_{\text{eff}})$ decreases monotonically with increasing d/Λ, as this parameter takes the values 0.40 [curve (1)], 0.41, 0.42, 0.43, 0.45, 0.46, 0.48, 0.49, 0.50, 0.55, 0.60, 0.65, 0.70, 0.75 [curve (14)].

$$\mathcal{L} = \frac{2\pi}{\lambda} \frac{20}{\ln(10)} 10^9 \, \mathrm{Im}(n_{\mathrm{eff}}), \qquad (2)$$

such that at fixed wavelength the losses and $\mathrm{Im}(n_{\mathrm{eff}})$ are directly proportional.

Figure 1 shows a sharp transition in the ratio of loss [$\mathrm{Im}(n_{\mathrm{eff}})$] versus wavelength on pitch (λ/Λ) for $d/\Lambda > 0.45$, whereas for $d/\Lambda < 0.45$ the transition becomes increasingly gradual, disappearing entirely near $d/\Lambda \simeq 0.40$. Note that the MOF structures of Fig. 1 all support a fundamental mode, with nonzero $\mathrm{Im}(n_{\mathrm{eff}})$, which we do not study here.

To investigate more fully the transition in Fig. 1, we studied a number of characteristic fiber parameters as a function of λ/Λ for various ratios d/Λ; in Fig. 2 we display five of these, for a geometry with $d/\Lambda = 0.55$. First, the loss is shown for 4-, 8-, and 10-ring geometries [curves (1), (2), and (3)], with the transition becoming more acute with an increasing number of rings but remaining at a fixed λ/Λ ratio. To make the transition more evident, we calculated the second derivative of the logarithm of the loss with respect to the logarithm of the pitch (Q; curve 4):

$$Q = \frac{d^2 \log[\mathrm{Im}(n_{\mathrm{eff}})]}{d^2 \log(\Lambda)}. \qquad (3)$$

This quantity exhibits a sharp negative minimum, giving an accurate value for the transition. Next, we show the effective radius [curve (5)]:

$$R_{\mathrm{eff}} = \frac{\iint r^2 S_z(r, \theta)\mathrm{d}r\mathrm{d}\theta}{\iint r S_z(r, \theta)\mathrm{d}r\mathrm{d}\theta}, \qquad (4)$$

where S_z denotes the real part of the component along the fiber of the Poynting vector and the effective area[8] [curve (6)], defined as

$$A_{\mathrm{eff}} = \frac{(\iint |E|^2)^2}{\iint |E|^4}. \qquad (5)$$

In both cases the integrals are taken over the structured cross section of the fiber only, because for leaky modes the fields diverge at infinity.[3] Parameters R_{eff} and A_{eff} change, respectively, by 1 and 2 orders of magnitude at the transition, with numerical errors causing the A_{eff} curve to be less smooth. Note that the quantity A_{eff} was relied on by Mortensen[2] in his study of the mode transition in MOFs.

The multipole method uses a Fourier–Bessel field expansion about each inclusion,[4] which, for the magnetic field in the local cylindrical coordinates of the inclusion, takes the form

$$H_z(r, \theta) = \sum_n B_n^{(H)} H_n(k_\perp r)\exp(in\theta), \qquad (6)$$

where typically $-5 \le n \le 5$. This lets us define the last indicative quantity [curve (7)] shown in Fig. 2: $\mathcal{M}$ is the ratio of the magnetic field monopole coefficient [$B_0^{(H)}$] to the magnetic field dipole coefficient [$B_1^{(H)}$] for a cylinder in the first ring of the

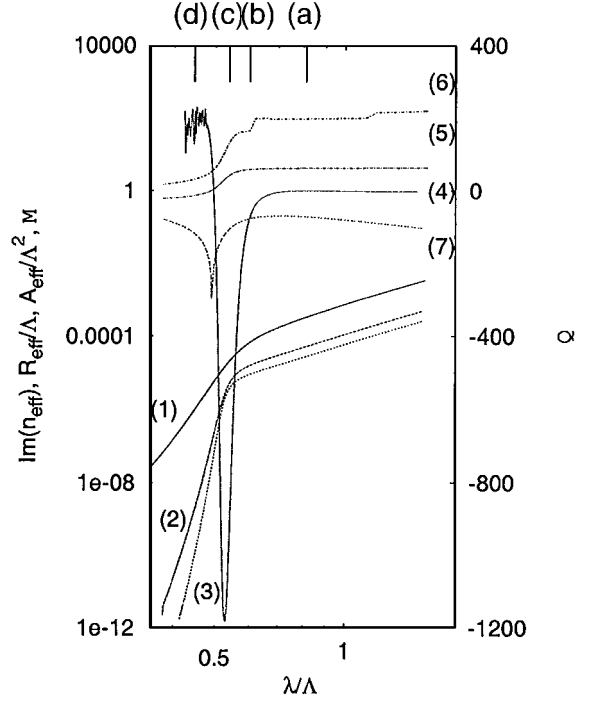MOF geometry. This ratio exhibits a well-defined minimum just below the transition. According to

Fig. 2. Variation of physical quantities during the transition for a MOF with $d/\Lambda = 0.55$ used at $\lambda = 1.55 \ \mu$m. Curves (1), (2), and (3) are $\mathrm{Im}(n_{\mathrm{eff}})$ for 4, 8, and 10 rings, and curves (4), (5), (6), and (7) are Q, R_{eff}/Λ, $A_{\mathrm{eff}}/\Lambda^2$, and $\mathcal{M}$, respectively, as defined in the text, for eight rings. Points (a)–(d) indicate the positions of the field plots in Fig. 3.
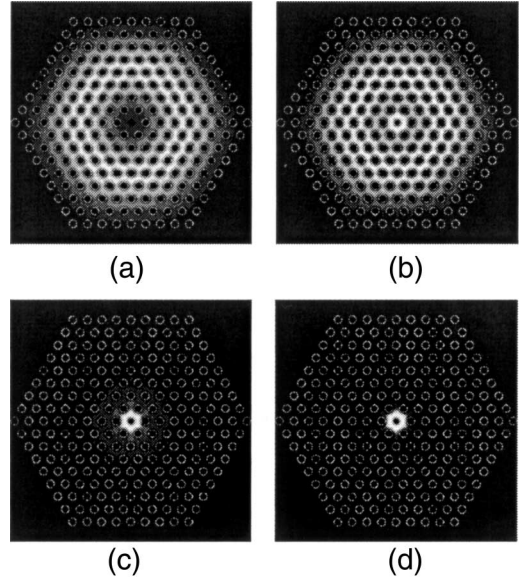

Fig. 3. Density plots of the real part of the z component of the Poynting vector of the second mode for four values of the pitch about the localization transition, for a structure of eight rings of holes with a diameter-to-pitch ratio $d/\Lambda = 0.55$. (a) Cladding filling state ($\lambda/\Lambda = 0.81$); (b), (c) transition states $\lambda/\Lambda = 0.599$ and $\lambda/\Lambda = 0.537$, respectively; (d) localized state $\lambda/\Lambda = 0.445$. The corresponding points are marked in Fig. 2.
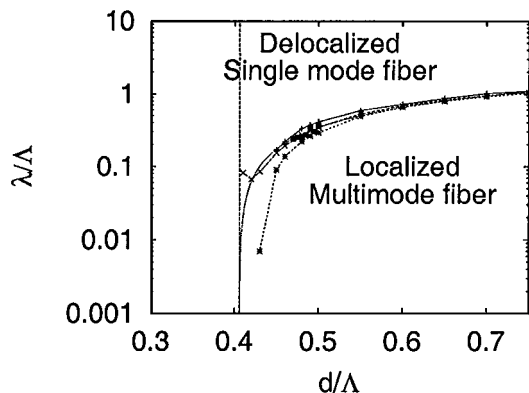
Fig. 4. Phase diagram of the second mode. The curves correspond to different definitions of the transition point: solid, A_{eff}; long-dashed, $\mathcal{M}$ minimum; short-dashed, $\mathcal{Q}$ minimum; dotted, fit from Eq. (6); squares, as in Ref. 2. In the lower region the second mode is confined and the fiber is therefore dual moded. The dashed vertical line shows the approximation to the limit of the endlessly single-mode regime.

Fig. 2, the nature of the mode changes quantitatively and qualitatively in a well-defined narrow region. We identify this transition with the cutoff of the mode.

In Fig. 3 we show the spatial variation of Poynting vector component S_z for the mode above [point (a), Fig. 2], during [points (b), (c)], and below [point (d)] the transition. Above the transition the mode is well described[9,10] as a space-filling cladding resonance. Its electric and magnetic fields are predominantly dipolar about each inclusion, and the magnitude of the Poynting vector decreases to small values in a smooth fashion both at the center and near the edge of the MOF structure. During the transition, its S_z distribution rapidly contracts [points (b), (c)] before stabilizing in a localized state [point (d)]. It is worth noting that, when they are localized, the losses seem to decrease exponentially with the number of rings, whereas when the mode is space filling, the decrease follows a power law.

We carried out similar analyses for 8-ring structures with 15 values of d/Λ ranging from 0.75 to 0.4. The results are shown in Fig. 4 together with the A_{eff} transition points from Mortensen,[2] which lie in the region from $d/\Lambda = 0.47$ to $d/\Lambda = 0.5$. Above $d/\Lambda = 0.45$, all criteria agree on a tightly defined transition curve. Below 0.45, the criteria become individually more or less difficult to apply because of the decreasing sharpness of the transition for finite systems.

Quantity $\mathcal{Q}$ from Eq. (3) in fact is the most sensitive indicator of the transition down to near the value where the transition ceases to occur. Using a log–log plot (not shown), we estimated that the transition disappears at $d/\Lambda = 0.406 \pm 0.003$. Below this ratio, $\mathcal{Q}$ remains positive everywhere.

Mortensen[2] and Broeng et al.[11] use a value of 0.45 for this significant point, but our investigation is for finite MOF geometries, whereas Mortensen used periodic boundary conditions. A best fit for the data ($\mathcal{Q}$ minimum) of Fig. 4 gives the single mode–dual-mode boundary as

$$\lambda/\Lambda \simeq \alpha(d/\Lambda - 0.406)^\gamma, \qquad (7)$$

with $\alpha = 2.80 \pm 0.12$ and $\gamma = 0.89 \pm 0.02$.

In conclusion, we have investigated whether mode number can be characterized in finite MOFs. We have shown that there exists a clear boundary between single- and dual-mode regions that can be determined by use of a range of criteria. At the boundary, the second mode changes rapidly from filling the entire cross section to being tightly confined about the defect, thus exhibiting a distinct cutoff.

References

1. T. A. Birks, J. C. Knight, and P. J. St. Russell, Opt. Lett. **22,** 961 (1997).
2. N. A. Mortensen, Opt. Express **10,** 341 (2002), http://www.opticsexpress.org.
3. A. W. Synder and J. D. Love, *Optical Waveguide Theory* (Chapman & Hall, London, 1996).
4. T. P. White, B. T. Kuhlmey, R. C. McPhedran, D. Maystre, G. Renversez, C. M. de Sterke, and L. C. Botten, "Multipole method for microstructured optical fibers. I. Formulation," J. Opt. Soc. Am. B (to be published).
5. B. T. Kuhlmey, T. P. White, R. C. McPhedran, D. Maystre, G. Renversez, C. M. de Sterke, and L. C. Botten, "Multipole method for microstructured optical fibers. II. Implementation and results," J. Opt. Soc. Am. B (to be published).
6. T. P. White, R. C. McPhedran, C. M. de Sterke, and M. J. Steel, Opt. Lett. **26,** 488 (2001).
7. For enhanced color versions of Figs. 1–4, see http://www.physics.usyd.edu.au/~borisk/physics/cutoff.html.
8. G. P. Agrawal, *Nonlinear Fiber Optics* (Academic, San Diego, Calif., 1995).
9. B. J. Eggleton, P. S. Westbrook, C. A. White, C. Kerbage, R. S. Windeler, and G. L. Burdge, J. Lightwave Technol. **18,** 1084 (2000).
10. M. Midrio, M. P. Singh, and C. G. Someda, J. Lightwave Technol. **18,** 1031 (2000).
11. J. Broeng, D. Mogilevstev, S. E. Barkou, and A. Bjarklev, Opt. Fiber Technol. **5,** 305 (1999).